JMEMS Letters

Response Speed Characterization of a Thermally Actuated Programmable Metamaterial

Chenyang Luo, Jonathan B. Hopkins, and Michael A. Cullinan, *Member, IEEE*

***Abstract*— This work details the experimental characterization of a MEMS thermal actuator, which constitutes a three-dimensional meso-robotic metamaterial lattice that can achieve actively controlled mechanical properties such as tunable stiffness. To achieve a target stiffness value via closed-loop control in a timeframe that is practical for most metamaterial applications, it is necessary that such actuators can rapidly respond to the controller's commands. In this letter, a fabricated thermal actuator experimentally demonstrates the ability to achieve desired stiffness values within 100s of milliseconds of receiving the command signal. The actuator can also maintain those stiffness values regardless of changing external loading conditions with acceptable accuracy. Thus, the results of this work prove that the metamaterial design can enable practical applications such as surgical tools that can change from compliant to stiff states as they perform their functions within the body and materials that can tune their natural frequencies to enable technologies that leverage resonant actuation such as steerable mirrors and optical switches. [2023-0150]**

***Index Terms*— Robotic metamaterials, tunable stiffness, thermal actuator, piezoresistive sensor, feedback control.**

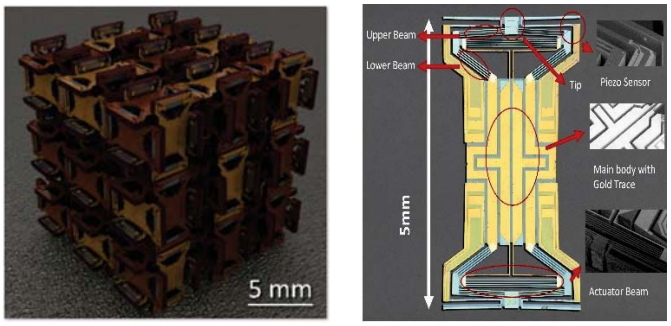

(a) (b)

Fig. 1. (a) Photo of a 3×3 × 3 metamaterial lattice of unit cells assembled using six individual actuator panels each. (b) Photo of the front side of the large-range version of the actuator panel that was experimentally characterized for this work.

I. Introduction

THE ability for a material to exhibit any desired combination of mechanical properties (i.e., Young's modulus, Poisson's ratio, shear modulus, etc.) on demand is revolutionary. To this end, researchers initially attempted to create materials that can be stimulated to achieve specific tunable properties using a large variety of different approaches. For example, shape memory polymers (SMPs) [1], [2] and magneto-rheological elastomers (MREs) [3] have shown promise as tunable components in a diverse set of industries. In the field of medical devices, SMPs demonstrate their versatility by adapting their stiffness to mimic natural tissues, enabling implants that dynamically replicate the mechanical profiles of surrounding biological structures [4], [5]. Similarly, magneto-rheological elastomers have found applications in haptic feedback systems, where they can be integrated into tactile interfaces to offer users varying levels of resistance or compliance during interactions with virtual objects. However, these types of material solutions often suffer from poor spatial resolution, slow response times, and limited tunability ranges.

More recently, it has become increasingly evident that one of the most promising approaches to create a material that can exhibit any desired combination of mechanical properties is by employing a lattice of tiny unit-cell-like robots that can be actively controlled within an active metamaterial (Fig. 1a) to respond to external loading scenarios with simple uploaded commands that collectively manifest as the desired lattice properties [6]. Such robotic metamaterials have recently demonstrated the ability to autonomously learn desired properties and behaviors as circumstances demand without programmers needing to upload the desired commands [7].

Thus far, however, it has yet to be demonstrated that any of the existing unit-cell robots, which constitute such metamaterials, possesses the micro/nano actuators and sensors that can exhibit the desired properties via closed-loop control with sufficient response speeds to enable the desired properties in any practical fashion. Fast response speeds become increasingly important for achieving uploaded dynamic properties and behaviors (e.g., focusing or redirecting the propagation of stress waves within the metamaterial's lattice). The typical human tactile response time is $\sim$ 600ms so a target response time (1τ) of 200ms was set for the device to allow the device to fully settle faster than the human perception limit. The actual response time of the thermal actuators in this system was measured to be $\sim$33.7 ms which is much faster than required for the desired applications. More details on this are provided in the supplementary information.

Thus, this work experimentally characterizes the response speeds of the most promising robotic metamaterial concept introduced by Luo et al. [6] to demonstrate that it can respond fast enough to enable practical metamaterial applications. A photo of a newly constructed 3×3 × 3 lattice of the concept is shown in Fig. 1a. Each 5-mm robotic unit cell consists of six actuator panels that are attached to an integrated circuit (IC) chip at their center. These IC chips

Manuscript received 11 August 2023; revised 14 September 2023; accepted 9 November 2023. Date of publication 22 November 2023; date of current version 5 February 2024. This work was supported in part by NSF under Grant NNCI-2025227 and Grant 1160494 and in part by the Air Force Office of Scientific Research (AFOSR) under Grant FA9550-22-1-0008. Subject Editor H. Fujita. *(Corresponding author: Michael A. Cullinan.)*

Chenyang Luo is with the Chandra Family Department of Electrical and Computer Engineering, The University of Texas at Austin, Austin, TX 78712 USA (e-mail: c11029lcy@gmail.com).

Jonathan B. Hopkins is with the Mechanical and Aerospace Engineering Department, University of California at Los Angeles (UCLA), Los Angeles, CA 90095 USA (e-mail: hopkins@seas.ucla.edu).

Michael A. Cullinan is with the Walker Department of Mechanical Engineering, The University of Texas at Austin, Austin, TX 78712 USA (e-mail: michael.cullinan@austin.utexas.edu).

This article has supplementary material provided by the authors and color versions of one or more figures available at https://doi.org/10.1109/JMEMS.2023.3332595.

Digital Object Identifier 10.1109/JMEMS.2023.3332595

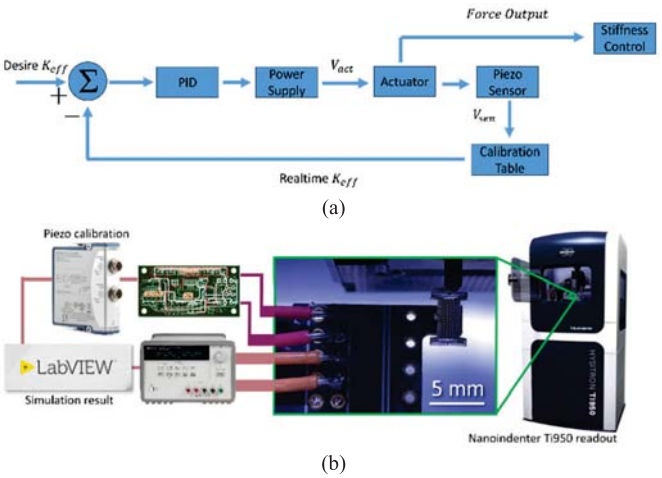

Fig. 2. A diagram of the connected closed-loop control system (a). A physical connection of the closed-loop control system with the verified nanoindenter (b).

control each panel's bidirectional thermal actuators and processes the measurements of their strain gauge sensors to leverage closed-loop control of the bulk lattice's properties as detailed in the previous publication [6]. For this work, a large-range version of the actuator panel (Fig. 1b) was fabricated to experimentally characterize its response speed. The geometric parameters and material properties of that specific design, referred to as Device 4 in the previous work [6], are provided in that letter.

II. Experimental Setup and Testing

Presented here is a comprehensive description of our experimental setup, focused on implementing a closed-loop communication system (Fig. 2a) via LabVIEW software, with a proportional-integral-derivative (PID) controller, to achieve tunable stiffness properties. The closed-loop system enables real-time feedback control, by precisely adjusting the actuator's response to external stimuli. The piezoresistive sensors in the MEMS chips that compose the robotic metamaterial are integrated into a Wheatstone bridge circuit and the amplified signal from this circuit is directed to a National Instruments readout system for high-speed data acquisition. This signal (V_{sens}), which represents displacement felt by the chip, is then converted into an effective stiffness (K_{eff}) and fed into the PID controller which adjusts to voltage into the actuator (V_{act}) and controls the force output by the system thus controlling the effective stiffness of the chip.

To validate piezo calibration, stiffness and displacement changes were simultaneously recorded using the nanoindenter and this dual data collection (Fig. 2b) verified the consistency of stiffness measurements from piezo sensors.

The transfer function used for the PID controller is given in Eq. 1 where V_{act} is the voltage drive on actuator, V_{sen} is the voltage output on piezoresistive sensor, K_{dev} is the intrinsic stiffness of the system and K_{act} is the stiffness added by the force produced by the actuator. C_1 and C_2 are both coefficients corresponding to actuator and sensor calibration.

$$\frac{V_{act}^2(t)}{V_{sen}(t)} = \frac{C_2(K_{eff} - K_{dev})}{C_1(K_{act})} \tag{1}$$

A particle swarm optimization (PSO) method is used to optimize the gains of the PID controller. In this optimization, a fitness function (Eq. 2) is used to define how well the system performs with different PID gain parameter combinations. Each particle in the PSO represents a set of PID gains (K_I, K_P, and K_D,) as its position in the search space.

$$Fitness = w_1\left(\frac{1}{Rise\ Time}\right) + w_2\left(\frac{1}{Settling\ Time}\right) - w_3\left(\frac{1}{Overshoot}\right) - w_4\left(\frac{1}{Control\ Effort}\right) \tag{2}$$

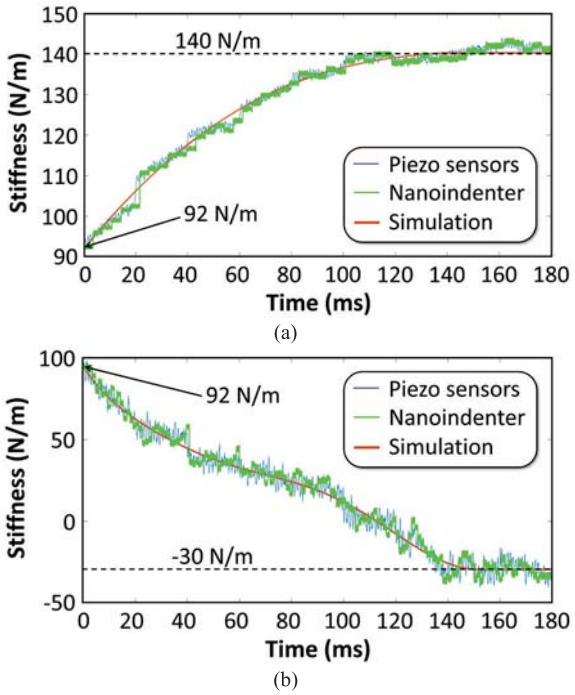

Fig. 3. (a) Testing result of desired 140 N/m positive stiffness reached in 120ms. (b) Testing result of desired −30 N/m negative stiffness reached in 140ms.

III. Results and Discussion

To evaluate the system's ability to tune its stiffness to any desired value, a consistent 1 μN force was applied to the device using a nanoindenter while simultaneously using the PID loop to control the stiffness of the device. The effective stiffness was then measured by the nanoindenter as the programmed stiffness of the device was changed. For example, the device in Fig. 3 has a natural stiffness of 92 N/m, but by utilizing the PID controller, we were able to achieve a programmed target stiffness of 140 N/m in approximately 120 ms with less than 6.4% error (Fig. 3a).

In the subsequent "negative stiffness" test with the same 92 N/m stiffness device we were able to achieve a programmed negative stiffness of −30 N/m with less than 7.1% error (Fig. 3b). Saturation of the PID controller took approximately 140 ms to manifest the negative stiffness response.

We also evaluated the stability of our device under diverse external conditions with the aim of investigating the impact that altering the external forces acting on the system has on the measured stiffness of the programmed device. To run this test, we varied the external force applied to the device from 1 μN to 4 μN and simultaneously monitored the displacement of both the device and the nanoindenter throughout these adjustments. To evaluate the device performance across a range of stiffness values, we chose one programmed stiffness close to the natural stiffness of the device (90 N/m) and one programmed stiffness significantly above the natural stiffness (120 N/m). We then measured the device's ability to maintain its programmed stiffness over the range of forces applied to the device. Our results show that the device was able to maintain its stiffness regardless of

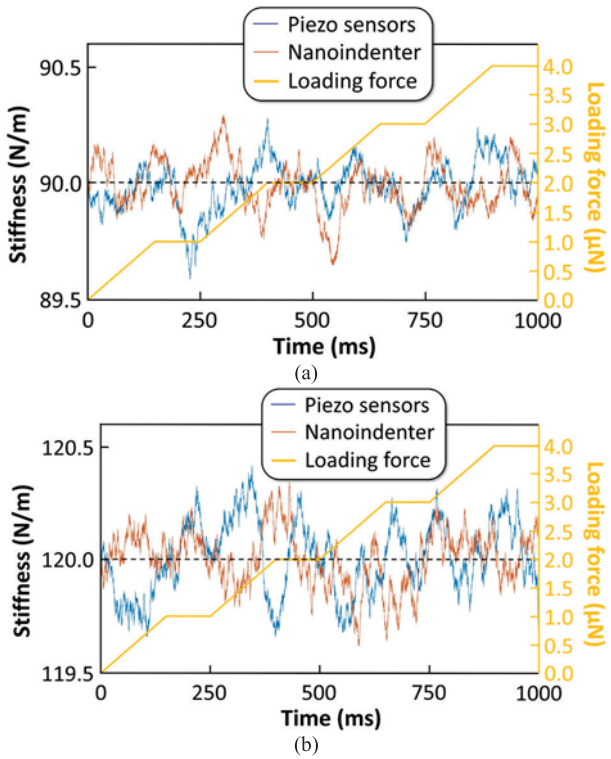

Fig. 4. (a) Stability test at (a) 80 N/m and (b) 120 N/m with varying force ranging from 1 μN to 4 μN.

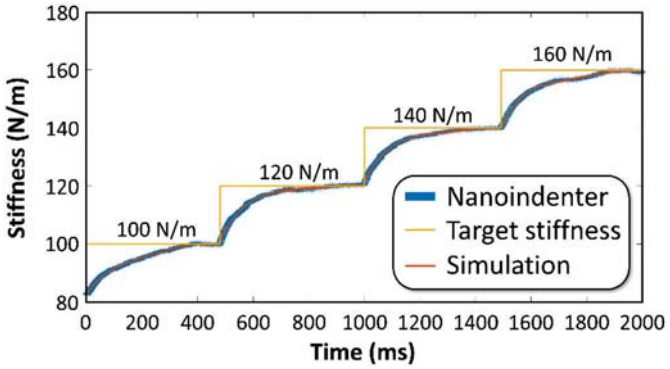

Fig. 5. Programmed and achieved stiffnesses demonstrating the ability of the device to change its stiffness over time.

outside forces or the value of the programmed stiffness. For example, in the 90 N/m programmed-stiffness test, the nanoindenter measured a stiffness of 89.4 $\pm$ 0.4 N/m over the full force range (Fig. 4a) and in the 120 N/m programmed stiffness test, the nanoindenter measured a 118.9 $\pm$ 0.2 N/m over the full force range (Fig. 4b). Overall, we observed that the stiffness was maintained at the desired level with fluctuations of less than 0.5%.

To ascertain the device's precision and accuracy in swiftly responding to disparate desired stiffness values, we set up an experiment where rapid adjustments in the programmed stiffness of the device were made while the nanoindenter maintained a constant 1 μN force on the device. Four distinct desired stiffness magnitudes of 100, 120, 140, and 160 N/m were chosen for this test. From these tests we learned that the system was able to achieve the desired stiffness within approximately 350 ms (Fig. 5) with less than 5% error between the programmed and measured stiffness values. These tests demonstrate the apparatus's steadfast and coherent self-regulation within the confines of imposed temporal constraints.

IV. Conclusion

This work demonstrates the ability of mm-scale robotic metamaterials to achieve desired, time-varying stiffness properties including negative stiffnesses. The success of this robotic metamaterial lies in the precise calibration and design of a closed-loop control system, which enables real-time stiffness adjustments with a rapid response time of less than 120 ms in some cases, meeting stringent design requirements.

References

[1] A. Lendlein and R. Langer, "Biodegradable, elastic shape-memory polymers for potential biomedical applications," *Science*, vol. 296, no. 5573, pp. 1673–1676, May 2002, doi: 10.1126/science.1066102.

[2] R. Xiao and W. M. Huang, "Heating/solvent responsive shape-memory polymers for implant biomedical devices in minimally invasive surgery: Current status and challenge," *Macromolecular Biosci.*, vol. 20, no. 8, Aug. 2020, Art. no. 2000108, doi: 10.1002/mabi.202000108.

[3] V. Kumar, S. Park, D. Lee, and S. Park, "Mechanical and magnetic response of magneto-rheological elastomers with different types of fillers and their hybrids," *J. Appl. Polym. Sci.*, vol. 138, no. 37, p. 50957, Aug. 2021, doi: 10.1002/app.50957.

[4] D. Habault, H. Zhang, and Y. Zhao, "Light-triggered self-healing and shape-memory polymers," *Chem. Soc. Rev.*, vol. 42, no. 17, p. 7244, Sep. 2013, doi: 10.1039/c3cs35489j.

[5] C. I. Idumah and S. R. Odera, "Recent advancement in self-healing graphene polymer nanocomposites, shape memory, and coating materials," *Polymer-Plastics Technol. Mater.*, vol. 59, no. 11, pp. 1167–1190, Jul. 2020, doi: 10.1080/25740881.2020.1725816.

[6] C. Luo et al., "Design and fabrication of a three-dimensional meso-sized robotic metamaterial with actively controlled properties," *Mater. Horizons*, vol. 7, no. 1, pp. 229–235, Jan. 2020, doi: 10.1039/c9mh01368g.

[7] R. H. Lee, E. A. B. Mulder, and J. B. Hopkins, "Mechanical neural networks: Architected materials that learn behaviors," *Sci. Robot.*, vol. 7, no. 71, Oct. 2022, Art. no. eabq7278, doi: 10.1126/scirobotics.abq7278.